ACS NANO

www.acsnano.org

ARTICLE

Bioinspired Camouflage Fibers with Computer Vision-Guided Chromatic Adaptation

Luyao Huang, Tingyu Cheng, Xianzhe Zhang, Haichao Zhang, Tejonidhi Deshpande, Yuanqiao Li, Zhi Xu, Gregory D. Abowd, Yun Fu, Yongmin Liu, Josiah Hester, Jun Li, and Hongli Zhu*

Cite This: https://doi.org/10.1021/acsnano.5c01492

Read Online

ACCESS | Metrics & More | Article Recommendations | Supporting Information

ABSTRACT: The development of intelligent camouflage systems demands advanced materials and control strategies for dynamic environmental adaptation. Here, we demonstrate a bioinspired camouflage system using hydroxypropyl cellulose (HPC), a cellulose derivative that forms cholesteric liquid crystals with mechanically tunable structural colors. By integrating HPC fibers with computer vision-assisted control, we achieve autonomous color matching with the environment through precise mechanical manipulation. Our system employs computer vision and a custom-designed wavelength-value (WV) mapping algorithm to analyze surroundings and control fiber tension, enabling direct modulation of the reflected wavelength. The closed-loop control system achieves color matching with less than 5% error at room temperature and maintains over 95% accuracy across temperatures from 15 to 35 °C. The HPC fibers exhibit reversible color transitions spanning the visible spectrum (400−700 nm). This integration of sustainable biomaterials with computer vision-guided mechanical control demonstrates an alternative approach for advanced camouflage applications, including military concealment and anticounterfeiting technologies.

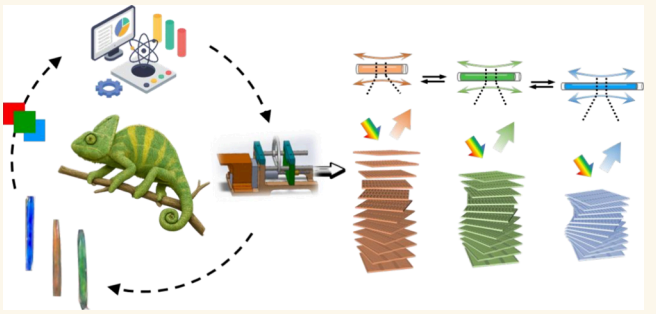

KEYWORDS: *structural colors, chromatic adaptation, hydroxypropyl cellulose, computer vision, artificial intelligence*

INTRODUCTION

With the advancement of modern technology, there is a growing demand for camouflage technology to be intelligent, reliable, sustainable, and versatile, catering to a wide range of military applications and everyday needs. In nature, many birds, chameleon and mammals exhibit specialized color adaptation mechanisms, allowing them to alter the color of their feathers or skin in response to environmental and temporal changes.[1−5] This helps them blend into their surroundings and achieve camouflage. Inspired by nature, researchers have increasingly focused on developing materials exhibiting variable structural colors for purposes such as equipment concealment, privacy protection, and information encryption.[6−8] Structural coloration emerges from the interference between visible light and a material's submicron structure, generating vibrant, precisely controlled colors.[9,10] Unlike traditional pigmentation, structural coloration is highly durable, making it well-suited for adaptive camouflage across diverse environments. The future of smart camouflage demands more than just color changes. Variable structural color materials, integrated with computer vision and structural control, could enable real-time adaptive responses to environmental stimuli. Such fusion harnesses both the physical agility of robots—their precise motion control and force generation—and computer vision's capacity for instruction processing, problem-solving, and autonomous decision-making, offering applications across diverse industries or even everyday applications. Integrating variable structural color-changing materials with control and computer vision not only facilitates specific camouflage objectives but also introduces cognitive capabilities, paving the way for innovative design paradigms in intelligent camouflage technology.

While prior research has demonstrated chameleon-inspired technologies using liquid crystals,[11] metallic nanostructures,[12] or thermochromic polymers,[13] these approaches often lack sustainability, adaptability, or scalability. In contrast, the use of natural biomass as a biodegradable, renewable material introduces a significant advancement in addressing environ-

Received: January 23, 2025
Revised: April 28, 2025
Accepted: April 30, 2025

Downloaded via NORTHEASTERN UNIV on May 16, 2025 at 18:26:13 (UTC).
See https://pubs.acs.org/sharingguidelines for options on how to legitimately share published articles.

© XXXX American Chemical Society

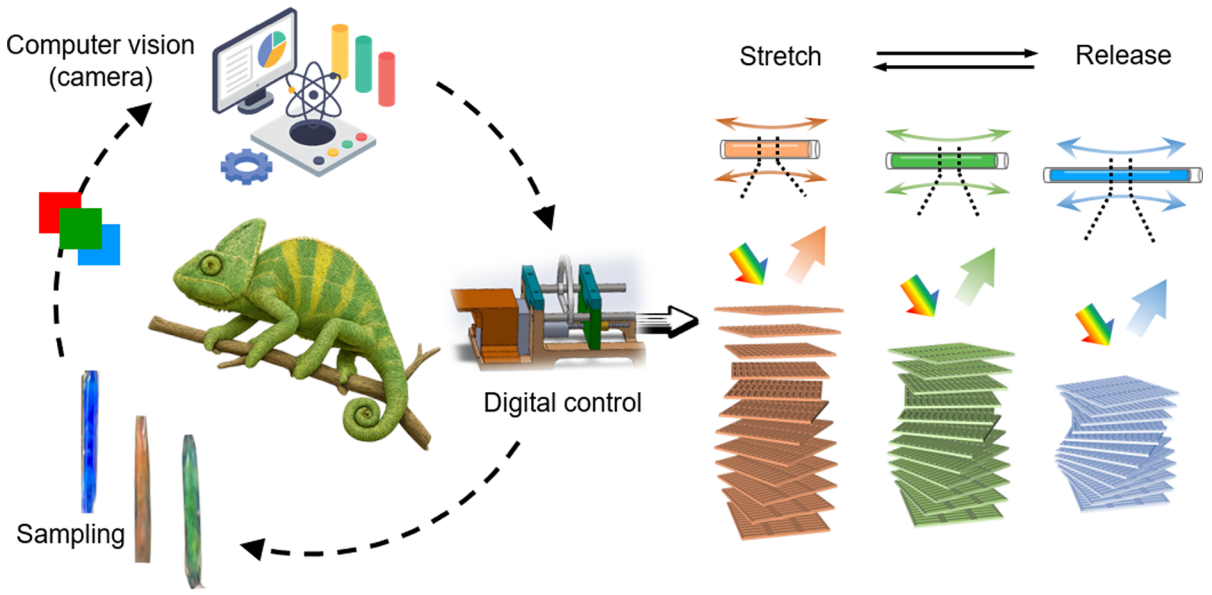

Figure 1. Schematic illustration of the HPC-based camouflage fiber system. The system consists of a mechanically adaptive HPC fiber that changes structural color in response to applied force, computer vision for environmental color detection, and AI-driven control for automated color matching. The integrated system enables dynamic camouflage adaptation through real-time wavelength analysis and mechanical control.

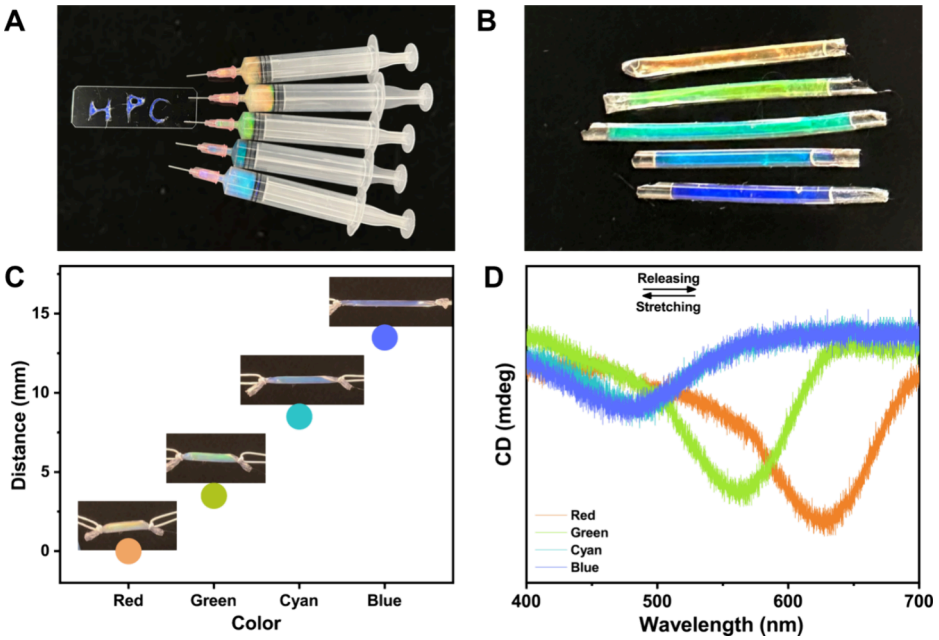

Figure 2. Multiple structural colors of the skin materials. (A) HPC gel with multiple structural colors; (B) HPC gel loaded in PDMS tubes to form HPC fibers with multiple structural colors; (C) HPC fibers with different structural colors as a function of stretch length; and (D) CD signals of HPC fibers at different stretch lengths.

mental concerns while maintaining functional versatility. One example is hydroxypropyl cellulose (HPC), a natural derivative of cellulose. When dissolved in common solvents, HPC forms cholesteric liquid crystal phases that can precisely replicate colors. Its reversible color changes, rapid responsiveness, and tunable structural properties make it particularly suitable for camouflage applications. However, there is no literature on HPC camouflage, where fine control of the structural color is used to create camouflage fibers. We address this challenge through the development of comprehensive closed-loop systems that integrate materials, cameras, computer vision-assisted system, and machine control for complete environmental sensing, analysis, and adaptive response. Incorporating HPC as the primary camouflage color, integrating it into the robot, analyzing captured information with AI algorithms, responding through autonomous system, and transmitting back to the computer for iterative comparison until the objective is attained represents a significant advancement in technology.

This study presents the development of structural color camouflage fibers capable of accurately mimicking the colors in their surroundings. To achieve this, HPC gels with structural colors were fabricated, encapsulated within polydimethylsilox-

https://doi.org/10.1021/acsnano.5c01492
ACS Nano XXXX, XXX, XXX−XXX

ane (PDMS) tubes and integrated into an original robotic model created by our research team (refer to Figure 1). Leveraging the visual input from Raspberry Pi HQ Camera to enhance environmental perception, the camouflage system analyzes environmental surrounding patterns, differentiates between ego-robotic pixels and the background, and determines the control signal by optimizing its own color. This is accomplished by directing the robot motor to manipulate the tension of the HPC fibers accordingly. Utilizing a stepper motor based sliding mechanism, the camouflage system optimizes the motor control signals in a structural wavelength reflection control loop to adjust the fibers colors. The alterations in the color of the HPC fibers stem from modifications in their internal molecular structure as they undergo stretching, inducing changes in their response to light polarization. To establish the direct algorithmic control of molecular structural color, we define a wavelength-value (WV) space to bridge the molecular structure to color and perceive molecular wavelength through pixels. Moreover, the adaptable nature of the HPC robot enables its operation across varying temperature ranges, from a high (35 °C) to a low (15 °C), rendering it a promising candidate for applications in anticounterfeiting protocols and military equipment. Unlike conventional systems, the integration of computer vision in this study ensures real-time, context-aware responses, overcoming limitations of predesigned patterns seen in traditional robots.

RESULTS AND DISCUSSION

Characterization of Structural Colors in HPC Gels. We developed the core material of the cholesteric biomass camouflage fibers, known as the HPC color-developing gel. HPC dissolves in water and self-assembles into ordered and stable periodic lamellar structures at concentrations of 60−70 wt %. The structural color of this gel can be controlled by adjusting the concentration of HPC and adding polyethylene glycol (PEG).[14] The rationale behind this mechanism is that the polarity of water or PEG induces alterations in the continuous periodic structure of HPC, thus modifying the reflected wavelength of light. The formulation is designed to enhance the structural color of HPC gels. Various HPC gels with distinct structural colors were produced by blending HPC, PEG, and water using a planetary mixer, as depicted in Figure 2A. From top to bottom, these gels are 65 wt % HPC gel in orange, 68 wt % HPC/PEG gel in orange, 67 wt % HPC gel in green, 68 wt % HPC gel in blue-green, 69 wt % HPC gel in blue (cyan), and 70 wt % HPC gel in blue purple ("HPC" font). All gels exhibit fluidity, enabling easy loading into syringes and efficient extrusion. To enhance the mechanical properties of the HPC gels, we encapsulated them with PDMS, valued for its high transparency. Figure S1A−C (in the Supporting Information) show that the prepared PDMS transparent tubes are bendable, rollable, and stretchable. Due to the fluidic property of the HPC gels, it can be easily loaded into hollow PDMS tubes via a syringe to produce fibers in various colors, as demonstrated in Figure 2B. Once filled with the HPC gel, the PDMS tubes retain excellent bendability and curling ability, as shown in Figure S1D.

Moreover, for intelligent camouflage fibers, it is crucial that the HPC fiber responds to background colors. Therefore, a study on the color variations during stretching motions is imperative. The PDMS ends encasing the HPC gel were tied and subjected to equal forces to induce deformation. Observations from Movie S1 reveal that the color of the HPC fiber transitions from orange-red to green, cyan, and ultimately blue as the stretching distance increases. Conversely, reducing the deformation reverses the color sequence from blue to cyan, green, and eventually red. This phenomenon occurs because HPC gels possess a unique ability to undergo stretching, which dynamically alters their structural color. As illustrated in Figure S2, the process of stretching and subsequent release modifies the helical spacing between HPC molecules. This spacing adjustment directly influences the wavelengths of light reflected by the gel, resulting in a noticeable color shift that is perceptible to the naked eye. Consequently, the color of the HPC gel changes in response to mechanical manipulation, showcasing its potential for applications where visual feedback or responsive color adaptation is desired. Figure 2C presents data illustrating the linear relationship between structural color changes and stretching distances. As stretching distances increase, colors transition from red to green to blue. Notably, this color transformation process is reversible. Thus, HPC fibers can effectively respond to mechanical stretching, adapting their colors to the environment. To further support this reversible color-shifting behavior, we characterized the mechanical performance of the HPC fibers. As shown in Figure S3, the fibers exhibited elastic deformation over to 80% strain, with a Young's modulus of ∼11.6 kPa. These results confirm that the fiber maintains sufficient mechanical flexibility and structural integrity during repeated stretching, enabling robust and stable color modulation in dynamic environments. In addition, we evaluated the long-term mechanical durability of the system through cyclic deformation tests. As presented in Figure S4, the HPC fiber retained consistent structural color over 50 stretch−release cycles, with no observable hue shift or mechanical degradation. This indicates that the cholesteric architecture remains intact under repetitive actuation, supporting the fiber's reliability for sustained operation in practical adaptive camouflage applications. To complement color observations, the circular dichroism detection of HPC fibers is crucial. The structural coloration of photonic materials is controlled by selectively reflecting visible light. The De Vries law can be utilized to estimate the corresponding reflection wavelength (λ), as following eq 1[15]

$$\lambda = n_{avg} P \cos\theta \tag{1}$$

where n_{avg} refers to the average refractive index of the cholesteric material; P denotes the helical pitch, representing the repeating distance of the cholesteric periodicity; and θ is the angle between the reflected light and the cholesteric helix axis. The cholesteric phase's corresponding λ at a consistent viewing angle depends on n_{avg} and P, influenced by various factors such as molecular weights, concentrations, and molecular interactions among multicomponent.[16,17] Therefore, different stretch distances can produce different structural colors in HPC fibers. Figure 2D displays the circular dichroism (CD) plots of orange 65 wt % HPC fibers at ambient temperature (25 °C) across various stretching distances. As the HPC fiber is stretched, the wavelength gradually shortens, causing a shift toward the blue end of the spectrum. Upon release, the color reverts to red, and the wavelength increases. Changing the amount of HPC gel in the optical path aperture during stretching results in variations in the strength of the CD signal, without affecting HPC's intrinsic right-handed property. This enables the incorporation of HPC fibers into machine

https://doi.org/10.1021/acsnano.5c01492
ACS Nano XXXX, XXX, XXX−XXX

components. These material properties form the foundation for the robotic system's adaptive capabilities, as detailed in subsequent sections discussing computer vision-assisted segmentation, control algorithms, and experimental outcomes.

Artificial Intelligence Camouflage Algorithm for HPC Camouflage Fibers. AI plays a crucial role in enhancing the capabilities of HPC camouflage fibers by enabling dynamic systems that autonomously adapt to changing environments. By leveraging advanced computer vision-guided system, HPC camouflage fibers can overcome traditional limitations, achieve higher adaptability, and efficiently interact with their surroundings. Although soft robots are capable of displaying predesigned active camouflage patterns, such as pixelated motifs on skin,[18] most still lack the ability to achieve real-time adaptive camouflage. A key limitation lies in the often-overlooked challenge of dynamically generating appropriate skin patterns in response to environmental changes. Consequently, soft robots are typically restricted to predefined patterns, limiting their ability to respond flexibly and blend seamlessly into their surroundings based on real-time sensory input. While perception capabilities in soft robotics have advanced significantly, few studies have focused on developing systems that enable rapid, adaptive camouflage in response to changing environments. To address this, we, for the first time, introduce a computer vision-assisted approach that leverages the ability to perceive and interpret background patterns, incorporating this understanding into control loops to mimic the background and blend seamlessly into their surroundings effectively. As illustrated in Figure 3, in the initial state, the

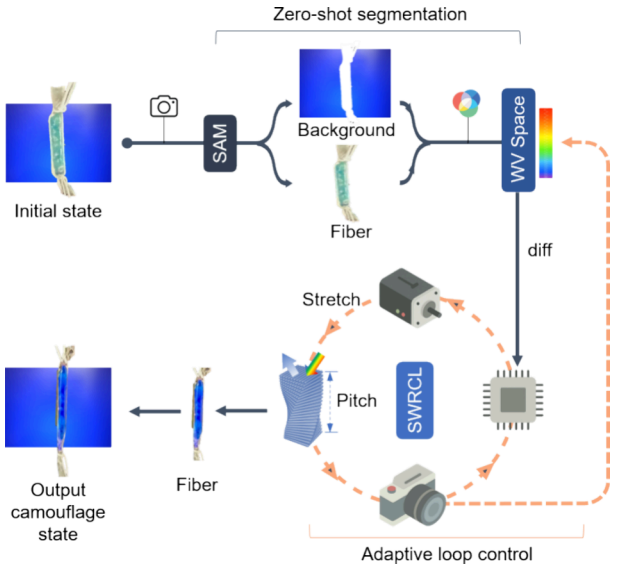

Figure 3. Illustration of structural wavelength reflection control loop.

system's process begins with the camera capturing both the background and the fiber as the foreground. The segmentation model then separates the input images into foreground and background components; we applied a pretrained zero-shot segmentation model (SAM[19]) to ensure that the segmentation model can adapt easily to different backgrounds without the need for predefined application scenarios during data collection, allowing for flexibility across environments. This process can be formulated as,

$$I_{seg} = F_{sam}(I_{in}) \tag{2}$$

where F_{sam} is the zero-shot segmentation model. I_{in} and I_{seg} are the input image and segmentation mask of the foreground fiber, respectively. Please note I_{seg} is the segmentation mask, represented as a binary matrix (with values of 0 and 1), indicating the foreground and background regions. Further segmentation is achieved by

$$I_{fiber} = I_{seg} \times I_{in} \tag{3}$$

$$I_{env} = (1 - I_{seg}) \times I_{in} \tag{4}$$

where I_{fiber} and I_{env} are the pixels representing the foreground fiber and background, respectively.

To enhance the capability of camouflage robots to mimic their environment accurately, we need to define and calculate their similarity between the fiber and background by measuring the distance between their pixels for the control module. The motivation for this approach is rooted in the observation that HPC fibers undergo a change in microstructure when subjected to stretch control, allowing them to reflect specific wavelengths of light. These changes are crucial for achieving effective camouflage. To effectively bridge the gap between microstructural changes and AI algorithms, we naturally adopt wavelength as a key metric. This allows us to measure the camouflage distance—the visual discrepancy between the fiber color and the background color. By focusing on this aspect, we gain direct control over the microstructural wavelength adjustments necessary for optimal camouflage. Building on this concept, we introduce a WV space, where the reflecting wavelength serves as the foundation for measuring visual similarity in the spectrum of wavelengths, aiming to deceive the human eye. The similarity $S(M_1, M_2)$ is calculated as

$$S(M_1,\ M_2) = \mathcal{L}_2(\text{wavelength}(M_1),\ \text{wavelength}(M_2)) \tag{5}$$

Here, M_1 and M_2 represent two materials, wavelength(*) is the wavelength reflected by material *, and $\mathcal{L}_2$ is the $L2$ norm.[20]

However, directly calculating the reflection wavelength of a material is difficult. Fortunately, we found that the hue in the HSV color space has a direct relationship with the dominant wavelength according to Grassmann's law,[21] as shown in eq 6, and can be linked to the RGB pixel values in eq 4:

$$H = (650 - \text{wavelength}) \times \frac{240}{650 - 475} \tag{6}$$

$$H = \begin{cases} \left(0 + \dfrac{G - B}{MAX - MIN}\right) \times 60, & \text{als } R = MAX \\ \left(2 + \dfrac{B - R}{MAX - MIN}\right) \times 60, & \text{als } G = MAX \\ \left(4 + \dfrac{R - G}{MAX - MIN}\right) \times 60, & \text{als } B = MAX \end{cases} \tag{7}$$

Here, R, G, B is the color channel of input images in RGB space.

So, we can calculate the wavelength from pixels by combining eqs 3, 4, 6, and 7,

$$\text{Wavelength}(M) = 650 - H(I_M) \times \frac{(650 - 475)}{240} \tag{8}$$

https://doi.org/10.1021/acsnano.5c01492
ACS Nano XXXX, XXX, XXX−XXX

where the $H(I_M)$ is the hue of material M, and $wavelength(M)$ is the wavelength reflected by material M.

We then measure the dominant wavelength from the wavelength spectrum in the WV space. By combining eqs 5 and 8, the WV space distance $S(M_{fiber}, M_{env})$ of the foreground fiber and background environment can be defined as

$$S(M_{fiber},\ M_{env}) = \frac{(650 - 475)}{240} \times (H(I_{env}) - H(I_{fiber})) \tag{9}$$

Specifically, the displacement can be either positive or negative, aligning with the control direction of the motor steps in the control loop. In practice, we replace $\frac{(650-475)}{240}$ with a hyperparameter λ for better loss convergence.

Finally, the background and foreground pixels are mapped into the WV space, and the calculated distance is fed into the Structural Wavelength Reflection Control Loop (SWRCL). The SWRCL adjusts the pressure applied to the fiber through motor steps until the WV space distance between the fiber and background converges below a predefined threshold. Upon convergence, the SWRCL applies the appropriate force to stretch the fiber, effectively camouflaging it to match the background, allowing the robot to blend seamlessly into its environment, as demonstrated in the camouflage results.

Cholesteric Flexible Fibers for Sustainable Camouflage. With the segmentation and control algorithms established, the next step involves applying these principles to real-world camouflage tasks, demonstrating the system's accuracy and responsiveness under varying conditions. The cellulose derivative HPC is utilized as a substrate for sustainable camouflage fibers. Our research indicates that HPC has the capability to form colorful structure-colored gels with water and can maintain vibrant structure colors across a broader concentration range. For the fabrication of camouflaged fibers, we specially selected orange (65 wt % HPC) and green (67 wt % HPC) fibers, which were tested against different backgrounds including blue, showcasing their responsiveness to environmental colors. The color transformation of HPC fibers in response to the background color at room temperature is illustrated in Figure 4. Despite varying shapes of plump and deflated HPC fibers, the structural color of the fibers remains consistent, showing no significant change in apparent color. This is crucial for maintaining effective camouflage without the need for constant adjustment.

In detail, as visible in Figure 4A and supplementary videos (Movies S2–S7), the robotic system initially identifies the colors of the background and fibers (e.g., yellow background and orange fibers at time T0). The AI algorithm then segments the pixels of both entities using eqs 3 and 4. Next, the model converts RGB values into Hue values through eq 7, and calculates the current and target spectral wavelength values using eq 8. An optimization process is applied to manipulate the microstructure of fiber to control the reflection wavelength. Within the control loop, the model measures the wavelength distance between the fiber and background through eq 9. Subsequently, a robotic arm is activated to execute stretching actions on the HPC fibers, manipulating the motor to move in 1 mm intervals, applying force to the fiber and modifying its internal molecular structure. After each action, the fibers are retrieved, analyzed, and the wavelength distance is recalculated in WV space, continuously adjusting the internal microstructure until convergence is achieved. As observed at T1 of

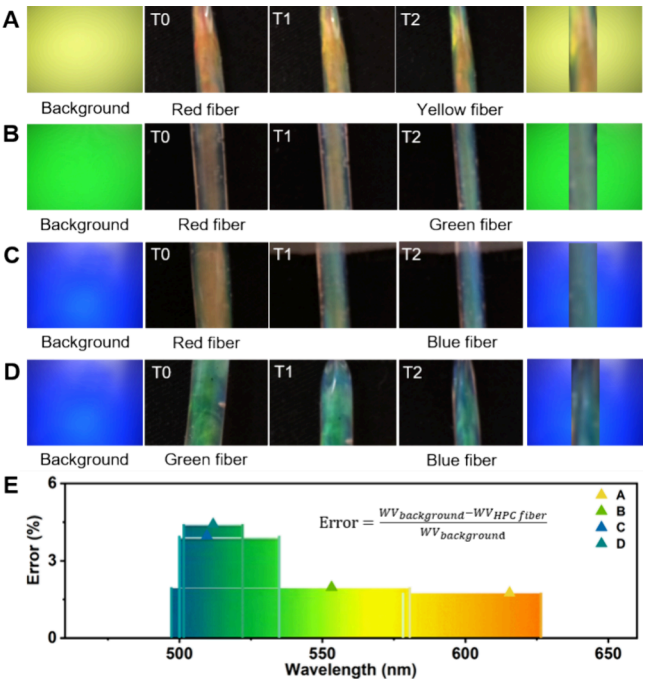

Figure 4. Camouflage performance with fast and stable controllability. (A) Red fiber turns into yellow fiber based on the yellow signal; (B) red fiber turns into green fiber based on the green signal; (C) red fiber turns into blue fiber based on the blue signal; (D) green fiber turns into blue fiber based on the blue signal; and (E) error of HPC fibers corresponding to different color signals. T0 represents the HPC fiber in the initial state, T1 represents the HPC fiber in the intermediate state, and T2 represents the HPC fiber in the end state. The total system response time for these transitions is measured as follows: (A) 12.953 s, (B) 12.342 s, (C) 10.962 s, and (D) 13.069 s. These times account for signal processing and mechanical actuation delays.

Figure 4A, the fiber hue shifts between orange and yellow. At this stage, the model continues to measure the wavelength distance and maintains the control loop, directing the robotic arm to persist in functioning until the difference in wavelength between the fiber and the background is less than 5%. Examination of the color information on the final HPC fiber and the background color yielded from the computer (refer to Table S1 of the Supporting Information) reveals that the wavelength of the yellow background color is 604.86 nm, while the wavelength of the HPC fiber in T2 is 615.44 nm. The error between the two wavelengths is calculated at 1.75%, signifying the successful accomplishment of the camouflage objective.

Figure 4B transitions to a green background, where the camouflage test continues with the orange HPC fibers. The computer replicates the steps and analysis from the yellow background test, with an adjustment in the number of iterations to encompass a broader color spectrum from orange to green. This implies that the elongation of the helical pitch of HPC fibers stretched over greater distances, as compared to those in their original state at the same HPC concentration, can be attributed to the flexibility of the self-assembled HPC molecule structure under tension. Additionally, we explored the potential of HPC fibers to camouflage against a blue visible light background, showcased in Figure 4C,D. The dynamic camouflage of HPC fibers was observed transitioning from initial orange and green colors to blue, facilitated by computer

https://doi.org/10.1021/acsnano.5c01492
ACS Nano XXXX, XXX, XXX−XXX

interaction. The functionality of the HPC variable structure color mechanism allows for mechanical forces to induce internal structural changes. For each fiber image at different states, we extracted the pixel- wavelength values and plotted pixel histograms using a step width of 0.2 nm (see Figure S5 in the Supporting Information). This approach allows a precise characterization of the wavelength distribution across the fiber surface. The results reveal that the pixel distributions for nearly all captured images exhibit an approximately normal distribution, suggesting that the reflected color is relatively uniform and concentrated, rather than scattered or patchy. Moreover, the mean wavelength deviation remains within a narrow and acceptable range under all tested background scenarios, confirming that the color tuning process leads to consistent and visually coherent camouflage.

Through rigorous performance assessment, we calculated the error for each camouflage, demonstrating in Figure 4E that all errors were kept below 5%. In addition to accuracy, the system's response time was quantified for different camouflage cases (Figure 4). Measured from the moment the environmental color is detected (T0) to the final state (T2), response times are all in the tens of seconds. These times include image processing, AI-based wavelength matching, and mechanical actuation, demonstrating an efficient adaptation cycle. It is noteworthy that enhancing the camouflage speed is feasible by refining the code and increasing the mechanical bed step length, with scalability across various applications. Moreover, we synthesized photonic fibers by injecting HPC gels into vacant PDMS tubes using a syringe, resulting in cylindrical fibers exhibiting consistent colors at similar viewing angles, albeit with minor inconsistencies. These irregularities could stem from the formation of localized disordered domains, potentially influenced by nonuniform evaporation kinetics and shear alignment during tube loading.[22] Although these fibers share the same cholesteric structure with HPC, their pitches may vary. However, by averaging the hue values across different pixels within the measurement region, such variations can be largely minimized, thereby reducing the impact of these irregularities.

Temperature-Independent Camouflage Fibers. Our camouflage fibers concept enables various electronic devices to function autonomously in outdoor settings. The chromatic properties of HPC are temperature-sensitive, allowing modulation of its structural color in response to ambient temperature changes. Specifically, the structural color shifts toward red as temperature rises and toward blue as temperature decreases, attributable to alterations in helical pitch resulting from changes in HPC intermolecular repulsion. Therefore, alongside evaluating the responsiveness of HPC fibers to room temperature ambient conditions, we conducted assessments under varying temperature conditions to ascertain the operational behavior of HPC fibers. To examine the thermal stability of HPC under different ambient temperatures, we selected orange HPC fibers (68 wt % HPC) at 35 °C and blue-green HPC fibers (65 wt % HPC) at 15 °C, allowing them to equilibrate at ambient temperatures for 20 min before assessing their performance. In Figure 5A, captured at an ambient temperature of 35 °C, the initially orange HPC fibers demonstrated stretchability toward yellow against a yellow background, indicating a blue shift in visual color due to pitch shortening. Analysis of the data in Table S2 and Figure 5C of the Supporting Information revealed wavelengths of 618.60 nm for the final yellow HPC fiber and 604.83 nm for the

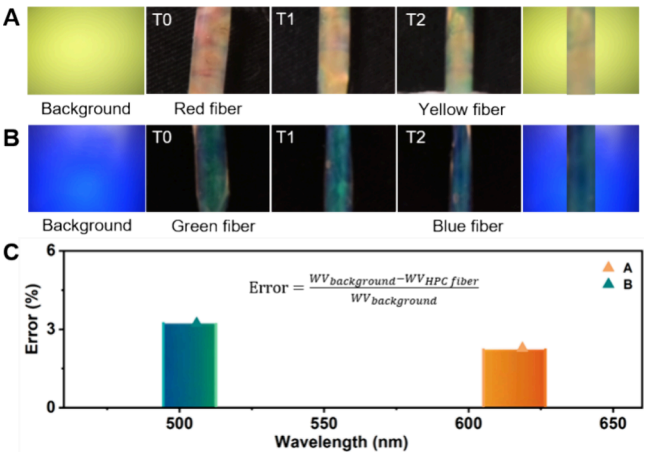

Figure 5. Effective camouflage with environmental adaptability. (A) Red fiber turns into yellow fiber based on the yellow signal of camouflage fibers in hot weather (35 °C); (B) green fiber turns into blue fiber based on the blue signal of camouflage fibers in cool weather (15 °C); and (C) error of HPC fibers corresponding to different environments. T0 represents the HPC fiber in the initial state, T1 represents the HPC fiber in the intermediate state, and T2 represents the HPC fiber in the end state. The response time for camouflage under environmental variations is measured as follows: (A) 12.667 s at 35 °C and (B) 16.726 s at 15 °C. These values reflect both AI-driven optimization and mechanical execution.

yellow background, with an error margin of 2.28%, a result of significant importance. Furthermore, experimentation was conducted on the HPC camouflage fibers in cold weather conditions with a blue background, resulting in autonomous color adaptation of the HPC fibers to blend into the blue environment, as displayed in Figure 5B. Analysis of the computer-generated data showed a final wavelength of 505.92 nm for the HPC fiber and 490.12 nm for the background, indicating an accuracy of 96.78%. These findings underscore the consistency of simulated diurnal operations with those at room temperature, highlighting the absence of a statistically significant correlation between temperature fluctuations and operational accuracy. Additionally, pixel wavelength histogram analysis during actuation (Figure S6) revealed consistent, unimodal wavelength distributions, confirming stable chromatic behavior under thermal or cold variation. The HPC intelligent camouflage fibers demonstrate the capability to operate continuously under realistic outdoor conditions, without loss of structural color performance or mechanical stability. This demonstrates strong potential for sustainable camouflage robotics. Beyond temperature-independent camouflage, an essential aspect of practical application is the ability to create functional pixelation within a 2D patterned structure. While traditional camouflage displays rely on electronic pixel control, our system achieves spatially tunable color modulation through the strategic arrangement of HPC fibers and membranes, as illustrated in Figure S7. Various configurations enable different levels of control: parallel fiber alignment allows synchronized or gradient-based transitions, braided structures facilitate localized deformation for independent color tuning, and membrane-based matrix designs introduce spatially controlled color shifts. These structured arrangements effectively mimic pixelated camouflage without requiring electronic control, demonstrating that a stretching-based

https://doi.org/10.1021/acsnano.5c01492
ACS Nano XXXX, XXX, XXX−XXX

structural color system can function as an adaptive and scalable camouflage material.

CONCLUSIONS

This work integrates HPC fibers, computer vision, and artificial intelligence to create an adaptive camouflage system with real-time and precise control over structural color. Our system exploits HPC's cholesteric liquid crystal properties to enable dynamic color changes through mechanical manipulation, achieving wavelength control across the visible spectrum (400−700 nm). Through our novel WV mapping algorithm, the system continuously analyzes environmental colors and translates them into mechanical adjustments, enabling real-time adaptation rather than relying on predefined patterns. This adaptive system addresses critical needs in dynamic camouflage technologies.

The HPC fibers, controlled by computer vision-assisted segmentation and mechanical feedback, demonstrate robust color-matching capabilities. Our computer vision system distinguishes target patterns from backgrounds using zero-shot learning, while the control system modulates internal fiber structure to achieve optimal color matching. Extensive testing validates the system's performance, showing over 95% color matching accuracy was achieved under algorithm-guided fiber actuation, validating the intelligent responsiveness and optical precision of the HPC-based camouflage system. Furthermore, the system maintained consistent hue matching performance across ambient temperatures ranging from 15 to 35 °C, with no observable optical drift or structural degradation during extended operation cycles. This performance enables effective camouflage adaptation across diverse environmental conditions. The outlined functionality establishes a framework for next-generation adaptive materials. While this proof-of-concept demonstrates the core technology, our vision extends to integrated systems where HPC fibers are woven into practical camouflage materials, such as fabric and soft robot. Future development will focus on miniaturization and wireless control to enhance portability and expand applications, particularly where camouflage technology intersects with artificial intelligence. These advances could transform fields from military concealment to anticounterfeiting measures, while establishing broader principles for intelligent material systems.

METHODS/EXPERIMENT

Materials. Hydroxypropyl cellulose (HPC, molecular weight 40,000) was obtained from Nippon Soda Co., Ltd. The polyethylene glycol (PEG) was purchased from Thermo Fisher and used directly without further treatment. Polydimethylsiloxane (PDMS, SYLGARD 184 Silicone Elastomer Kit) and mold release agent (ease release 200) were purchased from Fisher. All water was DI water.

HPC Gel Preparation. To prepare an HPC gel with a concentration of 67 wt %, 4 g of HPC and 1.88 g of water were weighed and placed into a sealed container. The mixture was stirred using a high-speed mixer (DAC 330-100 PRO, Flack-Tek, US) at 3500 rpm for 5 min. To remove air bubbles from the gel, the mixture was centrifuged at 4000 rpm for 30 min, resulting in a homogeneous and bubble-free gel. Building on our previous research, HPC/PEG hybrid gels with cholesteric phases were formulated using HPC, PEG, and water. Specifically, 5 wt % PEG (relative to the total HPC mass) was first dissolved in water, followed by the addition of 68 wt % HPC (relative to the total solution mass) to create the mixture. By adjusting the HPC content within the gel (ranging from 65 to 70 wt %), a spectrum of unique rainbow-like colors can be achieved. These gels serve as the base material for creating structurally colored fibers.

Polydimethylsiloxane (PDMS) Hollow Tube Fabrication. To fabricate hollow PDMS tubes, a mixture of PDMS (prepared with a 11:1 elastomer-to-hardener ratio) was thoroughly mixed and cast onto carbon fiber rods with a diameter of 1 mm. The assembled carbon fiber rod array was then baked vertically in an oven at 80 °C for 4 h to cure and solidify the PDMS. To facilitate easy removal of the cured PDMS from the carbon fiber rods, a release agent can be applied to the rods prior to casting. Once the curing process is complete, the solidified PDMS is carefully detached from the rods, resulting in the formation of hollow PDMS tubes.

HPC Fiber Fabrication. To fabricate HPC fibers of varying structural colors, disposable syringes were filled with distinct colored HPC gels and injected into the hollow PDMS tubes. After filling, the ends of the PDMS tubes were sealed to encapsulate the gel, forming HPC fibers with vibrant and varied structural colors. These fibers were designed to ensure durability and facilitate smooth traction during robotic operations.

Circular Dichroism Characterization. The expression to retrieve circular dichroism (CD) spectra is given by

$$\mathrm{CD} = \arctan\left(\frac{T_{\mathrm{LCP}} - T_{\mathrm{RCP}}}{T_{\mathrm{LCP}} + T_{\mathrm{RCP}}}\right) \tag{10}$$

where T_{LCP} and T_{RCP} are the transmittance of left-handed circularly polarized (LCP) and right-handed circularly polarized light (RCP) light through the sample, respectively.

A tungsten lamp was utilized as the broadband white light source. The emitted beam was collimated using two lenses and spatially filtered by two irises arranged to form a 4f optical system. Initially, a linear polarizer generated linearly polarized light, which subsequently passed through a quarter-wave plate to produce left- or right-handed circularly polarized light. Then it was focused on the sample with a convex lens (focal length of 50 mm) and collected with the same lens. A beam splitter directed the reflected light to the collection path of the setup, and a spectrometer (Horiba iHR550) was used to obtain the spectra. All experiments were conducted three times separately for left- and right-handed circularly polarized light.

Machine Control. For the mechanical controller, we developed a robotic linear slider equipped with a camera that can intelligently capture environmental colors and adjust the color of HPC fibers accordingly. This system also monitors the fiber's color changes in real-time. Most components, including the main base structure (see Figure S8 in the Supporting Information) and a moving carriage, were fabricated using 3D printing. The carriage has a 2-fold purpose, to securely hold the HPC fiber in place and to aid the linear motion utilizing the guide rods. The motion is driven by a bipolar stepper motor connected to a 200 mm lead screw. The reduction due to the lead screw enables the system to achieve a linear resolution of 1 mm and makes possible to apply a pulling force. Additionally, the core component for the system is the camera, mounted on a 3D-printed bracket, positioned at the top of the structure. The camera used (Raspberry Pi HQ Camera) has a Sony IMX477R stacked, back-illuminated sensor known for its high color accuracy, low noise, and high FPS capability.

Environmental Understanding with AI. To enable the camouflage robots fibers to rapidly respond to background color, our approach utilizes advanced AI techniques that enhance environmental understanding through tracking and segmentation. This allows for more precise control over the internal microstructure of materials to modulate reflected colors. Unlike traditional soft robots, which typically detect color using single-point color sensors or image processing methods limited to a fixed number of pixels within bounding boxes, our approach enables more comprehensive environmental analysis. Moreover, traditional supervised learning methods require large labeled datasets to cover diverse application scenarios, which often limits the adaptability of robotic systems. To overcome this, we employed a zero-shot learning approach leveraging recent advancements in large models, which allows the system to operate without the need for large, manually labeled data sets.

https://doi.org/10.1021/acsnano.5c01492
ACS Nano XXXX, XXX, XXX−XXX

For the input image sequence data, we utilized the SAM2[23] model to perform segmentation and track the pixels of both the background and the fibers. By calculating the distance between the background and fiber pixels in the wavelength-value (WV) space, we establish a wavelength-based metric to measure the similarity between the environment's color and the fiber's color. This metric serves as the basis for determining how well the fiber blends into the environment. It also aids in guiding the convergence of the control loop, allowing the HPC fibers to dynamically match their surroundings more effectively. This AI-driven environmental understanding ensures more efficient and adaptive camouflage in changing environments.

Measuring System Response Time. The response time of the system, defined as the duration from initial color detection (T0) to final convergence (T2), is primarily determined by the speed of the stepper motor that drives fiber deformation. While the system undergoes multiple stages, including image acquisition, color analysis, and mechanical actuation, the dominant factor influencing response time is the motor's speed, which can be adjusted to meet different application requirements. However, because the system design allows for straightforward speed adjustments, the response time can be optimized to accommodate various operational demands across different application scenarios.

ASSOCIATED CONTENT

Supporting Information

The Supporting Information is available free of charge at https://pubs.acs.org/doi/10.1021/acsnano.5c01492.

Supplementary figures (Figures S1−S8); tables with quantitative wavelength data and comparative studies (Tables S1−S3); and detailed descriptions of control system components and experimental setup (PDF)

Videos of the HPC fiber camouflage process (Movies S1−S7) (ZIP)

AUTHOR INFORMATION

Corresponding Author

Hongli Zhu − *Department of Mechanical and Industrial Engineering, Northeastern University, Boston, Massachusetts 02115, United States;* orcid.org/0000-0003-1733-4333; Email: h.zhu@neu.edu

Authors

Luyao Huang − *Department of Mechanical and Industrial Engineering, Northeastern University, Boston, Massachusetts 02115, United States; State Key Laboratory of Advanced Papermaking and Paper-based Materials, South China University of Technology, Guangzhou 510640, China*

Tingyu Cheng − *College of Computing, Georgia Institute of Technology, Atlanta, Georgia 30332, United States*

Xianzhe Zhang − *Department of Electrical and Computer Engineering, Northeastern University, Boston, Massachusetts 02115, United States;* orcid.org/0009-0000-9028-2870

Haichao Zhang − *Department of Electrical and Computer Engineering, Northeastern University, Boston, Massachusetts 02115, United States*

Tejonidhi Deshpande − *College of Computing, Georgia Institute of Technology, Atlanta, Georgia 30332, United States*

Yuanqiao Li − *Khoury College of Computer Sciences, Northeastern University, Boston, Massachusetts 02115, United States*

Zhi Xu − *Department of Electrical and Computer Engineering, Northeastern University, Boston, Massachusetts 02115, United States*

Gregory D. Abowd − *College of Computing, Georgia Institute of Technology, Atlanta, Georgia 30332, United States; Department of Electrical and Computer Engineering, Northeastern University, Boston, Massachusetts 02115, United States*

Yun Fu − *Department of Electrical and Computer Engineering, Northeastern University, Boston, Massachusetts 02115, United States; Khoury College of Computer Sciences, Northeastern University, Boston, Massachusetts 02115, United States*

Yongmin Liu − *Department of Mechanical and Industrial Engineering, Northeastern University, Boston, Massachusetts 02115, United States; Department of Electrical and Computer Engineering, Northeastern University, Boston, Massachusetts 02115, United States;* orcid.org/0000-0003-1084-6651

Josiah Hester − *College of Computing, Georgia Institute of Technology, Atlanta, Georgia 30332, United States*

Jun Li − *State Key Laboratory of Advanced Papermaking and Paper-based Materials, South China University of Technology, Guangzhou 510640, China;* orcid.org/0000-0001-8242-6184

Complete contact information is available at: https://pubs.acs.org/10.1021/acsnano.5c01492

Notes

The authors declare no competing financial interest.

REFERENCES

(1) Caro, T. The Adaptive Significance of Coloration in Mammals. *BioScience* **2005**, *55* (2), 125−136.

(2) Stuart-Fox, D.; Moussalli, A. Camouflage, Communication and Thermoregulation: Lessons from Colour Changing Organisms. *Philosophical Transactions of the Royal Society B: Biological Sciences* **2009**, *364* (1516), 463−470.

(3) Stuart-Fox, D. 6. Chameleon Behavior and Color Change. In *The Biology of Chameleons*; Tolley, K. A.; Herrel, A., Eds.; University of California Press, 2013; pp. 115−130.

(4) Wang, Z.; Guo, Z. Biomimetic Superwettable Materials with Structural Colours. *Chem. Commun.* **2017**, *53* (97), 12990−13011.

(5) Zimova, M.; Hackländer, K.; Good, J. M.; Melo-Ferreira, J.; Alves, P. C.; Mills, L. S. Function and Underlying Mechanisms of Seasonal Colour Moulting in Mammals and Birds: What Keeps Them Changing in a Warming World? *Biological Reviews* **2018**, *93* (3), 1478−1498.

(6) Arppe, R.; Sørensen, T. J. Physical Unclonable Functions Generated through Chemical Methods for Anti-Counterfeiting. *Nat. Rev. Chem.* **2017**, *1* (4), No. 0031.

(7) Waniek, M.; Michalak, T. P.; Wooldridge, M. J.; Rahwan, T. Hiding Individuals and Communities in a Social Network. *Nat. Hum Behav* **2018**, *2* (2), 139−147.

(8) Lou, D.; Sun, Y.; Li, J.; Zheng, Y.; Zhou, Z.; Yang, J.; Pan, C.; Zheng, Z.; Chen, X.; Liu, W. Double Lock Label Based on Thermosensitive Polymer Hydrogels for Information Camouflage and Multilevel Encryption. *Angew. Chem., Int. Ed.* **2022**, *61* (16), No. e202117066.

(9) Goodling, A. E.; Nagelberg, S.; Kaehr, B.; Meredith, C. H.; Cheon, S. I.; Saunders, A. P.; Kolle, M.; Zarzar, L. D. Colouration by Total Internal Reflection and Interference at Microscale Concave Interfaces. *Nature* **2019**, *566* (7745), 523−527.

(10) Zhu, X.; Yan, W.; Levy, U.; Mortensen, N. A.; Kristensen, A. Resonant Laser Printing of Structural Colors on High-Index Dielectric Metasurfaces. *Science Advances* **2017**, *3* (5), No. e1602487.

(11) Zhang, X.; Yang, Y.; Xue, P.; Valenzuela, C.; Chen, Y.; Yang, X.; Wang, L.; Feng, W. Three-Dimensional Electrochromic Soft Photonic Crystals Based on MXene-Integrated Blue Phase Liquid Crystals for

Bioinspired Visible and Infrared Camouflage. *Angew. Chem., Int. Ed.* **2022**, *61* (42), No. e202211030.
(12) Zhang, Y.; Zhu, H.; An, S.; Xing, W.; Fu, B.; Tao, P.; Shang, W.; Wu, J.; Dickey, M. D.; Song, C.; Deng, T. Chameleon-Inspired Tunable Multi-Layered Infrared-Modulating System via Stretchable Liquid Metal Microdroplets in Elastomer Film. *Nat. Commun.* **2024**, *15* (1), 5395.
(13) Guo, Q.; Zhang, X. A Review of Mechanochromic Polymers and Composites: From Material Design Strategy to Advanced Electronics Application. *Composites Part B: Engineering* **2021**, *227*, No. 109434.
(14) Huang, L.; Zhang, X.; Deng, L.; Wang, Y.; Liu, Y.; Zhu, H. Sustainable Cellulose-Derived Organic Photonic Gels with Tunable and Dynamic Structural Color. *ACS Nano* **2024**, *18* (4), 3627−3635.
(15) Shopsowitz, K. E.; Qi, H.; Hamad, W. Y.; MacLachlan, M. J. Free-Standing Mesoporous Silica Films with Tunable Chiral Nematic Structures. *Nature* **2010**, *468* (7322), 422−425.
(16) Wu, Y.; Wang, Y.; Zhang, S.; Wu, S. Artificial Chameleon Skin with Super-Sensitive Thermal and Mechanochromic Response. *ACS Nano* **2021**, *15* (10), 15720−15729.
(17) Li, D.; Wu, J.-M.; Liang, Z.-H.; Li, L.-Y.; Dong, X.; Chen, S.-K.; Fu, T.; Wang, X.-L.; Wang, Y.-Z.; Song, F. Sophisticated yet Convenient Information Encryption/Decryption Based on Synergistically Time-/Temperature-Resolved Photonic Inks. *Advanced Science* **2023**, *10* (5), 2206290.
(18) Kim, H.; Choi, J.; Kim, K. K.; Won, P.; Hong, S.; Ko, S. H. Biomimetic Chameleon Soft Robot with Artificial Crypsis and Disruptive Coloration Skin. *Nat. Commun.* **2021**, *12* (1), 4658.
(19) Kirillov, A.; Mintun, E.; Ravi, N.; Mao, H.; Rolland, C.; Gustafson, L.; Xiao, T.; Whitehead, S.; Berg, A. C.; Lo, W.-Y.; Dollár, P.; Girshick, R. Segment Anything. In *2023 IEEE/CVF International Conference on Computer Vision (ICCV)*; 2023; pp. 3992−4003.
(20) Hinton, G. E. A Practical Guide to Training Restricted Boltzmann Machines. In *Neural Networks: Tricks of the Trade: Second ed.*; Montavon, G.; Orr, G. B.; Müller, K.-R., Eds.; Springer: Berlin, Heidelberg, 2012; pp. 599−619.
(21) Grassmann, H. Zur Theorie Der Farbenmischung. *Annalen der Physik* **1853**, *165* (5), 69−84.
(22) Chan, C. L. C.; Bay, M. M.; Jacucci, G.; Vadrucci, R.; Williams, C. A.; van de Kerkhof, G. T.; Parker, R. M.; Vynck, K.; Frka-Petesic, B.; Vignolini, S. Visual Appearance of Chiral Nematic Cellulose-Based Photonic Films: Angular and Polarization Independent Color Response with a Twist. *Adv. Mater.* **2019**, *31* (52), No. 1905151.
(23) Ravi, N.; Gabeur, V.; Hu, Y.-T.; Hu, R.; Ryali, C.; Ma, T.; Khedr, H.; Rädle, R.; Rolland, C.; Gustafson, L.; Mintun, E.; Pan, J.; Alwala, K. V.; Carion, N.; Wu, C.-Y.; Girshick, R.; Dollár, P.; Feichtenhofer, C. SAM 2: Segment Anything in Images and Videos. *arXiv* August 1, 2024. .

https://doi.org/10.1021/acsnano.5c01492
ACS Nano XXXX, XXX, XXX−XXX